Swift Heavy Ion Induced Defect Study in Epitaxial n-Type CaAs from *In Situ* Hall Effect Measurements

M. Mikou, Régis Carin, P. Bogdanski, P. Marie

Swift Heavy Ion Induced Defect Study in Epitaxial n-Type GaAs from *In Situ* Hall Effect Measurements

M. Mikou, R. Carin (*), P. Bogdanski and P. Marie

LERMAT, CNRS (**), Université, 14050 Caen Cedex, France

(Received 27 July 1996, revised 10 March 1997, accepted 30 April 1997)

PACS.61 80.Jh – Ion radiation effects

PACS 61 72.Ji – Point defects (vacancies, interstitials, color centers,*etc.*) and defect clusters

PACS.61.72.Hh – Indirect evidence of dislocations and other defects (resistivity, slip, creep, strains, internal friction, EPR, NMR, *etc.*).

Abstract. — N-type (Si-doped, $N_D \approx 10^{17}$ cm^{-3}) GaAs epitaxial layers (MOCVD) are irradiated at 77 K with oxygen (0.163 GeV), krypton (5.15 GeV), xenon (5.73 GeV) and at 300 K with krypton (5.15 GeV). Hall effect measurements are performed, *in situ*, with increasing fluence A decrease of the electron concentration and a degradation of the Hall mobility, respectively due to trapping and to scattering on irradiation-induced point defects are pointed out. In the heavily doped layers, shallow donor impurities merge with the conduction band in distorted band tail. A simple two band conduction model is used as a simulation tool, which allows the carrier Hall concentration variation to be correctly fitted, as a function of both temperature and ion fluence The Hall mobility *versus* fluence variation at 77 K, which is mainly limited by screened ionized impurities and defects, is also simulated. From these simulations, the arsenic vacancy levels E_1 and E_2 are most likely to correspond respectively to single acceptor $(-/0)$ and single donor $(0/+)$ transitions. The introduction rates of induced defects (in particular V_{As}) are estimated: the total experimental introduction rate appears to be about 50% of the theoretical atomic displacement rate associated with nuclear collisions, independently of ion nature and of temperature. Although electronic stopping power S_e is about 2000 times larger than nuclear stopping power S_n, it is then suggested that irradiation-induced electronic excitation, in the investigated range $S_e = 1-12$ MeV/μm, has no effect on the degradation of n-type GaAs epitaxial layers

Résumé. — Des couches épitaxiées de GaAs de type n (dopage au silicium, $N_D \approx 10^{17}$ cm^{-3}) sont irradiées à 77 K avec des ions oxygène (0,163 GeV), krypton (5,15 GeV), xénon (5,73 GeV) et à 300 K avec des ions krypton (5,15 GeV). Les mesures d'effet Hall sont effectuées *in situ*, au fur et à mesure de l'accroissement de fluence. On observe une diminution de la concentration électronique et une dégradation de la mobilité de Hall, respectivement dues au piégeage et à la diffusion des électrons sur les défauts ponctuels créés par l'irradiation. Dans de telles couches fortement dopées, les niveaux d'impuretés dopantes (donneurs peu profonds) sont engloutis dans une queue distordue de la bande de conduction. Un modèle simple de conduction à deux bandes permet de simuler correctement les variations expérimentales de la concentration de Hall à la fois en fonction de la température et de la fluence des ions. On simule également les variations de mobilité de Hall avec la fluence à 77 K car à cette température, la diffusion est principalement due

(*) Author for correspondence (e-mail: rcarin@greyc ismra.fr)
(**) URA n° 1317, ISMRA

aux impuretés et défauts ionisés. A partir de ces simulations, il apparaît que les niveaux E_1 et E_2 de la lacune d'arsenic correspondent vraisemblablement aux transitions simple accepteur $(-/0)$ et simple donneur $(0/+)$. Une estimation des taux de production de défauts est effectuée . la quantité totale de défauts détectés est égale à environ 50 % du nombre théorique de déplacements atomiques provoqués par les collisions nucléaires, indépendamment du type d'ion incident et de la température. Bien que le pouvoir d'arrêt électronique S_e soit environ 2000 fois plus grand que le pouvoir d'arrêt nucléaire S_n, il semble que, dans la gamme explorée $S_e = 1-12$ MeV/μm, l'excitation électronique induite par l'irradiation n'ait pas d'incidence sur la dégradation des couches épitaxiées de GaAs de type n.

1. Introduction

Over the last years, studies of irradiation induced defects in semiconductor crystals have been widely developed. One aim of such studies is fundamental understanding of defect nature and of defect creation mechanisms. Much experimental work has been done to identify the point defects produced particularly in GaAs by electron irradiation [1]: the most widely studied defects are traps usually designated as E_1 (at $E_C - 0.045$ eV) and E_2 (at $E_C - 0.14$ eV) (Fig. 1a), which are generally thought to be related to the As vacancy V_{As}. The acceptor or donor nature of these traps has been a subject of discussion [2–5]. Recently, traps similar to $E_1 - E_2$ have been also detected after neutron irradiation of GaAs crystals [6].

Semiconductor irradiation studies also refer to electronic device technology, which involves ion implantation damage in crystals, and to damage which could be caused to devices by cosmic radiation in space applications. Both fundamental understanding and cosmic radiation simulation have encouraged investigations with swifter ions. The development of swift heavy ion accelerators, such as GANIL (Caen, France), allows the study of the nature and properties of damage produced by the passing of ions through crystalline material without implantation. In fact, the accelerated ions, with incident energy between 3 and 100 MeV per nucleon, are able to pass through 10 to 100 μm material thicknesses before stopping. Therefore, it is possible to use thinned samples in order to avoid implantation.

The semiconductor electrical parameters are modified by swift ion irradiation similarly to the case of implantation. The ion induced defects are associated with levels, located in the band gap, which trap electrical carriers present in the material. Thus, the carrier concentration and the mobility decrease with ion fluence. However, the defect creation mechanisms may be quite different from the case of implantation. For incident velocity larger than core electron velocities, very swift ions collide independently with the atomic nuclei of the crystalline matrix and with the electrons. Then, defect production may involve two separate mechanisms which are connected respectively with nuclear stopping power S_n and with electronic stopping power S_e Each collision (ion-nucleus or ion-electron) is simply described by the Rutherford formula which leads to two consequences: (i) if T_n is the amount of energy transferred to a nucleus during the collision, the Rutherford cross section is proportional to T_n^{-2} so that the small values of T_n are more probable and the mean value of T_n is relatively small (less than 500 eV for 5.73 GeV xenon ion in GaAs); (ii) because of the small electron mass, the electronic stopping power is much larger than the nuclear stopping power ($S_e \approx 2000 \times S_n$, with S_n values about keV/μm). Moreover, the mean free path of the incident ion between two effective nuclear collisions is larger than 0.1 μm: finally, every primary hard collision produces only a small cascade of about 5 to 8 atomic displacements (see Tab. I) and the swift ion induced damage consists of spaced point defects (and not clusters). However, the large electronic excitation due

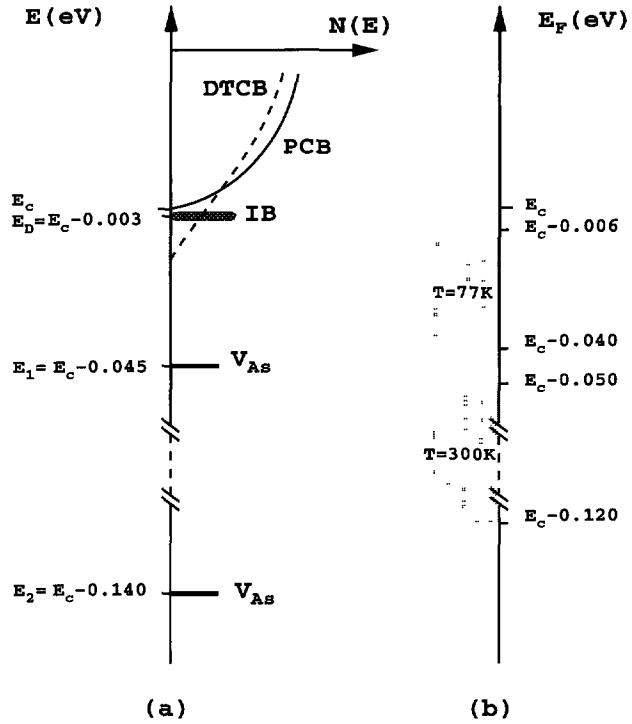

Fig 1. — a) Schematic representation of electron state density $N(E)$, in the upper part of the band gap, in 10^{17} cm^{-3} n-type doped GaAs. The E_1 and E_2 defect levels are related to the As-vacancy; the distorted tailing conduction band is pictured by the dashed line DTCB, for the simulations, the band tail is supposed to be concentrated at discrete average energy E_D, in a rough two band model (parabolic conduction band PCB and impurity band IB) b) Fermi level E_F variation intervals explored during irradiations performed at 77 K and at 300 K, for the present work.

Table I. — *Defect creation rate values (defects/ μm) deduced from the simulations of experimental Hall effect results: arsenic vacancy (η_{12}). other charged acceptors (η_{AI}), total rate ($\Sigma\eta_i$). For each irradiation, we also indicate several theoretical parameters calculated by TRIM computation: atomic displacement rate due to nuclear collisions (Ndpa/e), incident ion mean free path between two effective nuclear collisions (λ), mean number of atomic displacements for each ion hard collision (C), nuclear stopping power (S_n), and electronic stopping power (S_e).*

Incident ion nature (and Temperature)	η_{12} (μm^{-1})	η_{AI} (μm^{-1})	$\Sigma\eta_i$ (μm^{-1})	$Ndpa/e$ (μm^{-1})	λ (μm)	C	S_n (keV/μm)	S_e (MeV/μm)
O (77 K)	3.75	4	7.75	11.2	0.48	5.5	0 49	0.92
Kr (77 K : 300 K)	7.5	8	15 5	34	0.21	6.2	1.7	4.5
Xe (77 K)	22 1	23 6	45.7	91	0 095	7.5	5.3	11.6

to S_e may influence considerably damage production, either by creation of defects (large defect production is observed in some metals [7]), or by annealing [8]: according to the investigated material, different specific damage effects can also be observed (phase changes, amorphisation, plastic deformation) [9].

In the case of semiconductors, previous DLTS results have confirmed that swift ion induced

damage in Si [10], Ge [11,12], and GaAs [13] consists of point defects similar to irradiation by fast electrons. Resistivity measurements suggest that the electronic excitation has no influence on defect production in Si [14] and induces probably annealing in Ge and GaAs [15,16]. The study of GaAs may be particularly interesting because of the polar nature of this material: this could make GaAs sensitive to large electronic excitation. To determine the incidence of electronic excitation, quantitative studies are needed. In this paper, a quantitative estimation of defect creation rates in n-type GaAs is deduced from *in situ* Hall effect measurements during irradiation, by comparing simulated and experimental curves (carrier concentration and mobility *versus* ion fluence) Several ions corresponding to different values of S_e are used and, for every ion, we perform a comparison between the experimental defect production rate and the theoretical rate corresponding only to nuclear collisions, which allows the effect of electronic stopping power to be estimated.

To reach that goal, we used n-type doped ($N_D \approx 10^{17}$ cm^{-3}) epitaxial GaAs: in Section 2, we explain the advantages, for our study, of such material and we discuss the choice of the simulation model used for electron conduction. In Section 3, we describe the selected model and we test it for simulation of the characteristics of the material before irradiation. In Section 4, we simulate the Hall parameters of GaAs layers under irradiation, which allows the defect creation rates to be derived. Then, the electronic stopping power effect can be argued in Section 5

2. GaAs Material and Conduction Model Choice Reasons

Defect analysis in swift ion irradiated GaAs is deduced from Hall effect and conductivity measurements· our previous experiments [13, 16] have been carried out on thinned samples with thicknesses smaller than the ranges of the ions in the targets (less than 10 μm in some cases). The thinning techniques present two disadvantages for the analysis of defects produced by irradiations: first, the superficial layers of samples are degraded by mechanical polishing, as has been observed for Ge [17]; secondly, the fragility of the thinnest samples means that they need to be supported on solid substrates· this may induce an important strain and also cause uncertainty in the measured thicknesses of the samples. In this paper, the Hall effect experimental results are obtained for the first time on GaAs epitaxial layers where the thickness is known with good precision ($6 \pm 0\ 1$ μm). However, it is essential that implantation in the underlying substrate does not perturb measurements. This is the case for semi-insulating GaAs substrates which are used in our study: the implantation defect clusters may strengthen the insulating character of the substrates, but this does not influence the Hall effect and conductivity measurements in the epitaxial layers.

The use of epitaxial samples offers another advantage. their chemical and cristallographic quality is better than for previous thinned samples obtained from LEC materials [13]. The epitaxial layers have been grown at "École Polytechnique de Lausanne" (Switzerland), at 550 °C, on semi-insulating GaAs substrates (Cr-O doped), by the organometallic method (triethyl-gallium). Their n-type doping (Si) concentration N_D is approximately 10^{17} cm^{-3}. A small compensation exists in the layer: acceptor carbon was detected from photoluminescence spectra. The n-type doping was selected with a rather high value of carrier concentration (10^{17} cm^{-3}) because this choice allows the Fermi level to be located in the upper part of the gap during the irradiation for both 77 K and 300 K experiments (Fig. 1b). Thus, lower levels, which could be related to grown-in defects and to acceptor carbon impurity, keep their charge state constant and do not influence Hall parameter variations with neither temperature nor fluence. However, the arsenic vacancy charge state is dependent on E_F variation and the $E_1 - E_2$ levels largely influence the carrier trapping variation. The conditions are thus favourable for

the arsenic vacancy production under irradiation to be observed. indeed, it has been shown from previous DLTS results, obtained for n-type LEC GaAs, that swift ion irradiation creates more particularly the $E_1 - E_2$ levels [13].

However, the high doping of n-type GaAs presents a disadvantage as it is difficult to use an accurate conduction model in such material Indeed, the states of neutral shallow donors in GaAs were widely studied [18]: as a result of the small electron effective mass, the donor ionization energy is small (5.8 meV) and the Bohr radius is large ($\approx$ 10 nm in the ground state). For donor densities as low as 10^{15} cm^{-3}, the excited states of shallow donors overlap and merge with the conduction band, thus reducing the thermal activation energy of the donor ground state. As discussed in reference [19], when N_D increases, the quasi-continuum of excited states broadens and approaches the donor ground level When N_D exceeds about 10^{16} cm^{-3}, the quasi-continuum encompasses all states (excited and ground states): then, the impurity band formed from the donor levels merges completely with the conduction band. Thus, one no longer observes any carrier freeze-out, all the Si donors are ionized. However, the band tailing results in a distorted conduction band [20], and it is difficult to build a model which accounts for the carrier mobility variation in the band tail and which could predict the energy position of the band limit as a function of temperature.

A rough model was previously used to simulate Hall concentration variations (initially 2×10^{17} cm^{-3}) during 1 MeV electron irradiation performed at room temperature [5]. This model supposes that the conduction band is rigidly shifted downward by 0.015 eV, which means that the band tail limit stays at $E_C - 0.015$ eV, and that electron mass or mobility, in the distorted tail, are not modified with respect to parabolic conduction band· the Si doping states are then chosen at $E_C - 0$ eV, in the band. To our knowledge, this model was not previously used to predict mobility variation *versus* temperature or *versus* electron fluence. We tried to use this model to simulate our experimental results. However, it was impossible to obtain an acceptable fit for carrier Hall concentration and mobility *versus* fluence variations at 77 K This trial was not successful probably because the model is too simple and does not account for band tail distortion

Another simple model had been previously used in reference [21] to simulate electrical characteristics of n-type GaAs: the donor state overlapping was then supposed to result in impurity band conduction. This two band (conduction band and impurity band) model have allowed the temperature variations of both carrier Hall concentration and mobility to be correctly simulated, especially for $N_D < 10^{16}$ cm^{-3} [21]. For $N_D > 10^{16}$ cm^{-3} , the two band model is undoubtedly less realistic than the band tail model. However, we shall see that this model also gives acceptable fits for our experimental results. We believe that this result may be due to the model hypothesis that electron mobility is reduced in impurity band with respect to conduction band: this assumption may be a simple way to account for the band tail distortion. In that way, the two band model can be used for $N_D > 10^{16}$ cm^{-3} if the "impurity band" represents the low mobility band tail, which is then supposed to be concentrated at discrete average energy E_D (Fig. 1a).

In this paper, our aim is to estimate ion induced defect creation rates from simple simulation of Hall parameter variations. We shall show in Section 3 that the two band conduction model allows the carrier concentration *versus* temperature variation to be reasonably simulated for n-type 10^{17} cm^{-3} doped GaAs samples used in this study. This result validates the use of such a model as a simulation tool to describe the quantitative relation which exists between Hall carrier concentration and Fermi level position in highly doped n-type GaAs. The model simplicity may induce small systematical uncertainty for creation rate estimation. However, the determination of creation rate ratios, either for different temperatures, or for different ions, is fully significant.

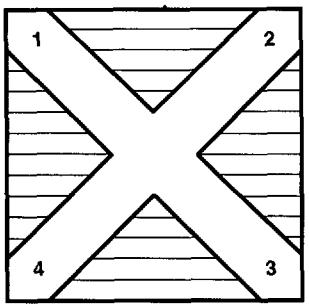

Fig. 2. — On an about 6 mm square cleaved substrate, the Greek cross shape sample is engraved in epitaxial layer by sandblasting The van der Pauw electrical measurement method uses four ohmic contacts labelled 1, 2, 3 and 4

3. Characterization of GaAs Epitaxial Layers Before Irradiation

Hall effect measurements are performed using the van der Pauw technique [22] We use a Greek cross shape for the samples which allows any geometrical correction to be avoided. The samples (Fig. 2) present four electrical contacts labelled 1, 2, 3, 4. $I_{\alpha\beta}$ indicates the direct current intensity flowing from α to β contacts, $V_{\gamma\delta}$ indicates the voltage difference between γ and δ contacts. A first measurement made with no magnetic field gives the resistivity, ρ, of the sample:

$$\rho = \frac{\pi}{\ln 2}\, d\, \frac{V_{14}^0}{I_{23}^0}$$

where d is the epitaxial layer thickness. A second measurement performed with a magnetic field, $B = 2.50 \times 10^{-2}$ T, perpendicular to the cross plane, gives the "Hall concentration", n_{H}, of the electrons:

$$n_{\mathrm{H}} = \frac{B\, I_{24}}{q\, d\, V_{13}},$$

where q is the elementary charge. Finally, the Hall mobility is deduced from previous measurements by:

$$\mu_{\mathrm{H}} = \frac{\ln 2}{\pi}\, \frac{V_{13}}{B\, I_{24}}\, \frac{I_{23}^0}{V_{14}^0}.$$

Figures 3 and 4 respectively represent experimental results of n_{H} and μ_{H} *versus* temperature, in the interval 77-300 K.

The simulations of these results use the two band model to give precisely the characteristics of the investigated material Precautions must be taken when interpreting quantitatively the results. It is well known that carrier scattering in the band is altered by the magnetic field: this explains the appearance in the expressions of n_{H} and μ_{H} of the dimensionless factor taking values between 1 and 2, called Hall factor r_{H}. The r_{H} value depends on relative importance of the various scattering mechanisms, temperature, carrier concentration and compensation ratio. Previous theoretical calculations [18,23] specify these variations: for the GaAs conduction band at 77 K and for a doping near 10^{17} cm^{-3}, r_{H} depends on the compensation ratio, and we assume an average value $r_{\mathrm{H}} = 1.2$ [18]; at 300 K, r_{H} drops rapidly to 1 for highest concentrations and we assume r_{H} value near 1.05. For the impurity band, we simply choose a Hall factor which value equals 1, reflecting quasi-metallic conduction [21]. The interest of the two band model is the introduction of two different carrier mobilities. For simplicity, the model states a relatively

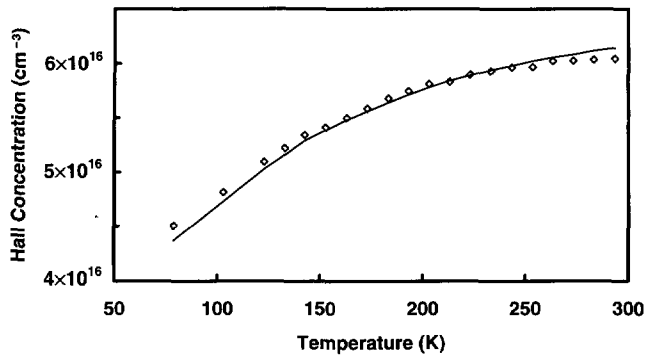

Fig. 3. — Experimental (dots) and simulated (line) variations of Hall concentration n_H *versus* temperature. The measurement is carried out before irradiation to characterize the material.

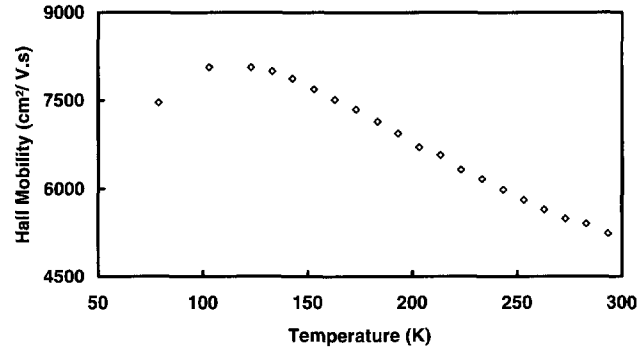

Fig. 4. — Experimental variation of Hall mobility μ_H *versus* temperature. The simulated result is not shown, because of the crudeness of the Matthiessen rule, since it overestimates the μ_H value by approximately 50% near the room temperature

crude hypothesis: we suppose a constant value of the ratio $W = \mu_B/\mu_C$, of respective electronic mobilities in the impurity band (μ_B) and in the conduction band (μ_C) [21]. Thus, the equations used for the simulation are:

$$n_H = \frac{(n_C + n_B W)^2}{n_C r_H + n_B W^2} \tag{1}$$

and

$$\mu_H = \frac{n_C r_H + n_B W^2}{n_C + n_B W} \mu_C, \tag{2}$$

where n_B and n_C are the electronic concentrations respectively in the impurity band and in the conduction band.

The n_C calculation is performed classically for a degenerate semiconductor by integrating the Fermi-Dirac function in a parabolic band. The Fermi level E_F is defined at each temperature by imposing the electrical neutrality condition; before irradiation, this reduces to:

$$n_C + n_B + N_A = N_D \tag{3}$$

with:

$$N_D - n_B = N_D\{1 + 2\exp[(E_F - E_D)/kT]\}^{-1}, \tag{4}$$

where k is the Boltzmann constant. The material contains acceptor compensative impurities (particularly acceptor carbon), with concentration N_A. Because of the E_F location in upper part of the gap, acceptor impurities are completely ionized. We assume that they are singly charged. N_D is the doping concentration (Si in donor position); the corresponding impurity band (in fact, the band tail) is assumed to be concentrated on effective energy E_D, which value is supposed to be approximately 3 meV under the bottom of the conduction band, for N_D close to 10^{17} cm^{-3} [21]

In this paper, the μ_C simulations are achieved by using the Matthiessen rule to combine the different contributions to carrier scattering. This simple calculation assumes that the contributions present the same energy variation or that only one contribution is preponderant. This is the case for 77 K experiments in highly doped GaAs where the mobility is mainly limited by screened ionized impurities and defects (contribution labelled μ_{ii}). However, we do not use our μ_C model at $T = 300$ K, because the mobility contribution μ_p due to scattering with phonons is about as important as μ_{ii} for concentrations near 10^{17} cm^{-3}. then, a more rigorous iterative calculation has previously shown [24] that the Matthiessen rule overestimates the electronic mobility in GaAs by approximately 50%.

Another mobility contribution is due to scattering by neutral impurities and defects. This contribution may be important particularly for hydrogenic centers such as neutral shallow donors in GaAs [25]. In fact, in the impurity band conduction hypothesis, or in the band tail model, the electrons are delocalized Thus for the μ_C calculation, all the donor atoms must be considered entirely ionized and consequently, there is no contribution of scattering by neutral impurities. Furthermore, for the irradiated material, we assume that the scattering by neutral induced defects produces no significant contribution. Finally, the μ_C calculation is performed only at 77 K, using the equation:

$$\mu_C^{-1} = \mu_p^{-1} + \mu_{ii}^{-1}, \tag{5}$$

where μ_p is the mobility in very pure GaAs, which is mainly limited by scattering with polar optical phonons [26] and where μ_{ii} is the contribution due to carrier scattering by screened ionized impurities and defects. This last contribution is described by the Brooks-Herring formula [18]:

$$\mu_{ii}(\mathrm{cm^2V^{-1}s^{-1}}) = \frac{2.12 \times 10^{18} T^{3/2}}{N_{ii}(\mathrm{cm^{-3}}) Z^2 [\ln(1+Y) - Y/(1+Y)]}, \tag{6}$$

with

$$Y = 1.11 \times 10^{14} \frac{T^2}{n(\mathrm{cm^{-3}})}.$$

(Z is the charge state of the ionized impurities or defects). The total electronic concentration which contributes to the screening is:

$$n = n_C + n_B. \tag{7}$$

Before irradiation, it reduces to $n = N_D - N_A$, and the total ionized impurity concentration is: $N_{ii} = N_D + N_A$

Three parameters of the model are unknown: W, N_D, N_A Their values are adjusted to make the simulated values of μ_H at 77 K, n_H at 77 K, n_H at 300 K coincide with the experimental ones. The values of the concentrations ($N_D \approx 10^{17}$ cm^{-3} and $N_A \approx 2 \times 10^{16}$ cm^{-3}) show that the material doping and the compensation ratio are of the same order of magnitude as the values obtained when assuming no impurity band and the constant value $r_H = 1$ [18, 24]. Concerning the mobility ratio, we obtain $W \approx 0\,2$. this relatively large value reflects a large contribution of the impurity band in the total conduction for $N_D \approx 10^{17}$ cm^{-3}. For smaller

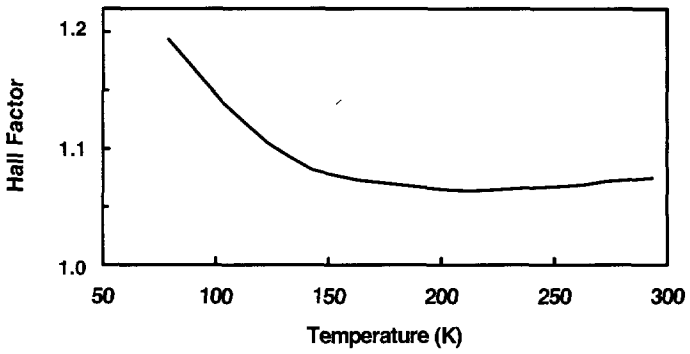

Fig 5 — Empirical variation of Hall factor r_H *versus* temperature deduced from simulation of Hall density $n_H(T)$ using the two band conduction model.

doping concentration $N_D \approx 10^{16}$ cm^{-3}, a smaller value $W \approx 0.05$ has been previously reported [21] The complete adjustment, by simulation, of the experimental curve $n_H(T)$ can be achieved (Fig. 3). It gives an empirical $r_H(T)$ variation which is represented in Figure 5: the shape of this curve is in good agreement with the theoretical calculations previously reported [23], which have been obtained for doping and compensation ratio close to ours.

In summary, the results have shown that the two band model equations describe correctly the Hall characteristics for n-type 10^{17} cm^{-3} doped GaAs. The material parameter values (W, N_D, N_A) have been derived. It is then possible to apply the model to the material under irradiation to simulate the variations of n_H(77 K), μ_H(77 K) and n_H(300 K). However, the variation of μ_H(300 K) under irradiation will not be interpreted in this paper because it would need a more elaborate calculation.

4. Behaviour of GaAs Layers Under Irradiation

Samples similar to those described in Section 3 have been irradiated at "Grand Accélérateur National d'Ions Lourds" (GANIL, Caen, France) by different swift ions: oxygen, krypton, xenon, with respective energies 0.163 GeV, 5.15 GeV and 5.73 GeV. The ion fluxes φ used are lower than 10^9 cm^{-2} s^{-1} and avoid any notable variation in the layer temperature which is fixed either at 77 K or at 300 K. The irradiation is intermittent, Hall effect measurements are performed during the interruptions of the beam. Figure 6 represents two examples of experimental variations of Hall concentration n_H *versus* fluence φt, obtained with the same ion, krypton, at the same energy 5.15 GeV, for the two irradiation temperatures 77 K and 300 K. The corresponding variations of the Hall mobility are represented in Figures 7 and 8. For each experiment, the irradiation is stopped when the sample becomes too resistant (over about 10 MΩ). Then, Hall parameters are no longer indicative of the bulk of the material, but are due to current losses at the surfaces of the device or in the measurement circuit. the experimental limit is obtained when Hall effect is no longer symmetrical with reversing magnetic field.

The simulations of these results are realized with the same hypothesis as in Section 3, assuming a constant value of W during irradiation, by adding the contributions of the irradiation induced defects. In fact, the considered variations correspond to moderate irradiation. For highest fluence, carrier concentration is larger than 10^{15} cm^{-3} , which means that the Fermi level always stays in the upper part of the band gap. Furthermore, from the Brooks-Herring formula (6), it can be shown that the experimental value μ_H(77 K), for highest fluence,

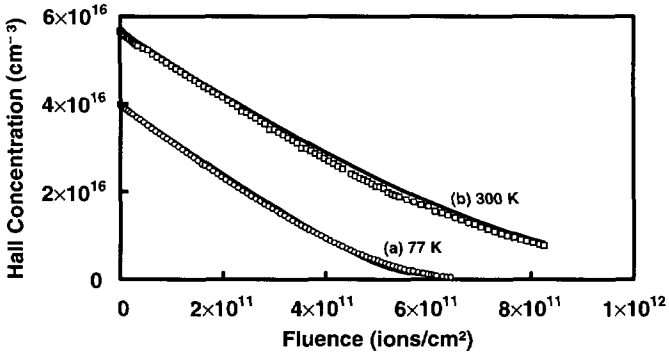

Fig. 6 — Experimental (dots) and simulated (lines) variations of Hall concentration n_H *versus* fluence (Kr ions, energy 5.15 GeV) for 77 K (a) and 300 K (b) irradiations. In fact, the simulated line corresponds to three superimposed curves obtained with different values of the defect creation rates, respectively for the three charge value transition hypothesis concerning the arsenic vacancy trap levels E_1 and E_2 (as in Fig 7).

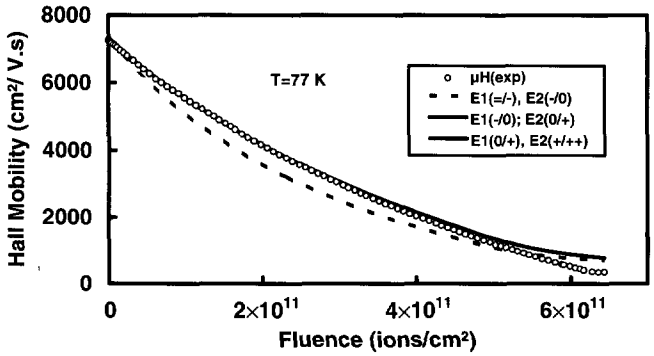

Fig. 7. — Experimental (dots) and simulated (lines) variations of Hall mobility μ_H *versus* fluence (Kr ions; energy 5.15 GeV) for 77 K irradiation (same sample as Fig. 6a) The three simulated curves (two of which are superimposed) correspond to the three charge value transition hypothesis concerning the arsenic vacancy trap levels E_1 and E_2

corresponds to densities of ionized defects, some 10^{17} cm^{-3}, which is of the same order as the density $(N_D + N_A)$ of ionized impurities present in the material. These observations suggest that the simulations can be realized with several approximations. First, the ion induced defect densities are low enough to allow the creation rates to be assumed constant with fluence Secondly, the r_H variation can be neglected at the beginning of the irradiation. However, for the highest fluence, the large compensation rate induced by irradiation may result in r_H variation up to 20% at 77 K [18]. Therefore, as the simulations are realized with constant r_H value, it is important that calculation fit experimental variations for low fluences rather than for higher fluences In particular, a reliable test for the simulation parameter adjustment is a good fit of the initial slopes of n_H and μ_H *versus* fluence curves. At last, because of E_F location in the upper part of the band gap, simulations need to know the defect level energies only for those which are up in the gap. Indeed, the defects are neutral or charged according to the relative positions of the Fermi level E_F with respect to the energy levels characterizing transitions to

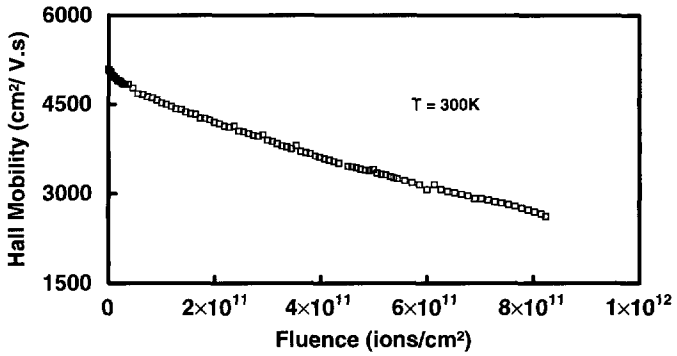

Fig. 8. — Experimental variation of Hall mobility *versus* fluence (Kr ions; energy 5 15 GeV) obtained for 300 K irradiation (same sample as Fig 6b).

a negative charge state (acceptor-level) or to a positive charge state (donor-level). From the variation of n_H during irradiation, one can calculate that the Fermi level varies in the range: $E_C - 0.006$ eV to $E_C - 0.04$ eV at 77 K and $E_C - 0.05$ eV to $E_C - 0.12$ eV at 300 K (Fig. 1b). In the fitting models, one then needs to consider only the charge state transitions associated to defects with ionization levels located in this energy range.

Previous DLTS studies have shown that the point defects produced by ion irradiation in semiconductors are the same as those produced by electron irradiation. Particularly, in n-type GaAs [13], the levels produced by ion irradiation in the upper part of the band gap are only the well known levels $E_1 = E_C - 0.045$ eV and $E_2 = E_C - 0.14$ eV. The other defects are probably also the same as for electron irradiation but our previous DLTS study has been performed for ion irradiated LEC GaAs [13] so that, excepted $E_1 - E_2$, the ion induced defects (with levels lower than $E_C - 0.3$ eV) were masked by native defects. In any case, it is not necessary, for the present simulations, to know these defects with levels located below $E_C - 0.3$ eV: for $E_F > E_C - 0.12$ eV, such defects are practically ionized if acceptors, and neutral if donors

The E_1 and E_2 levels are assigned to the same defect, the arsenic vacancy V_{As}. Its corresponding charge states have been a controversial topic: E_1 was first supposed to involve a double acceptor transition (= /−) [2]; then a double donor transition (+/ + +) was invoked for E_2 [3]. Recently positron annihilation experiments [4] have suggested that E_1 corresponds to a single acceptor (−/0) transition and E_2 to a single donor (0/+) transition. The same charge state hypothesis has previously allowed the Hall concentration variation to be correctly simulated for electron irradiation [5]. It will be seen that our best simulations of the Hall mobility variations under ion irradiation are also obtained with this hypothesis and that the single acceptor-single donor model is the more likely one for the arsenic vacancy. The other acceptor defects, which are totally ionized during irradiation, are supposed to be singly charged. This last hypothesis is not evident: some acceptor defects may be multicharged. Therefore, we have performed several tentative simulations for which a large fraction of the deep acceptor defects had been supposed doubly charged ($Z = 2$). However, because of the Z^{-2} factor in equation (6), multicharged ions result in strong mobility decrease, which always gave unacceptable fits.

The defect production rates, which are supposed to be constant during irradiation, are labelled η_{12} for V_{As}, and η_{AI} for all the other acceptor defects. Besides, donor defects, with deep energy levels, are probably produced, as for electron irradiation [1], but in the neutral state: they are ignored in our calculations. For a fixed fluence φt, the different defect concentrations are: $N_{12} = \eta_{12} \times \varphi t$ for V_{As}, and $N_{AI} = \eta_{AI} \times \varphi t$ for other negative ions. The concentrations of

the vacancy (with single acceptor - single donor hypothesis) in the different charge states are respectively:

$$N_{12}^{-} = \eta_{12}\varphi t\{1 + 2(1 + 0.5\ \exp[(E_2 - E_F)/kT])\exp[(E_1 - E_F)/kT]\}^{-1} \quad (8)$$

$$N_{12}^{+} = \eta_{12}\varphi t\{1 + 2(1 + 0.5\ \exp[(E_F - E_1)/kT])\exp[(E_F - E_2)/kT]\}^{-1}. \quad (9)$$

Then, the electrical neutrality condition can be written:

$$n_C + n_B + N_A + N_{12}^{-} + N_{AI} = N_D + N_{12}^{+}. \quad (10)$$

The simulation is conducted as in Section 3. The Fermi level position E_F is obtained from equations (4, 8-10): it imposes n_C and n_B values (Eq (4)). The mobility contribution μ_n is calculated from equations (6,7), with:

$$N_n = N_D + N_A + N_{12}^{-} + N_{12}^{+} + N_{AI}. \quad (11)$$

The n_H and μ_H values are finally deduced from equations (1, 2, 5), assuming that the r_H Hall factor does not vary during irradiation. The only unknown parameters are the defect production rates η_{12}, η_{AI}: their values are adjusted to realize the best simulations of the experimental variations of both n_H and μ_H *versus* φt at 77 K (Figs. 6a and 7). To verify the arsenic vacancy charge states, such calculations were also performed (with modified equations (8-11)) for the three charge state models. For the double acceptor hypothesis, the position of the Fermi level at 77 K induces the production of double negatively charged vacancies: because of the $Z = 2$ value in equation (6), the mobility decreases too rapidly with fluence, especially at the beginning of the irradiation (Fig. 7), and it is impossible to simulate correctly the μ_H variation for any values of the defect production rates. For the single acceptor-single donor hypothesis and for the double donor hypothesis, the vacancies are initially produced mainly in the single negatively charged state and in the neutral state, respectively: then the decrease of the mobility is slow and good agreement with the experimental variations can be obtained for the two models but with different values of η_{12} and η_{AI}. In the latter case (double donor), the η_{AI} value is almost two times the η_{12} value: we believe that this result is unconsistent with those obtained in previous electron irradiation studies [1] for which DLTS measurements showed that the arsenic vacancy is produced with a creation rate higher than for the other acceptor defects. So we believe that the single acceptor-single donor assumption is the most likely because of the value, about 1, obtained for the η_{12}/η_{AI} ratio, which is more consistent with the DLTS results. Thus, we come round to the conclusions obtained from positron annihilation experiments [4].

The irradiation temperature influence is now considered. Within the measurement uncertainty limit, the experimental n_H variation obtained for 300 K irradiation can be correctly simulated (Fig. 6b) using the same η_{12}, η_{AI} values as for 77 K irradiation. This result indicates that the charged defects are created with similar concentrations for 77 K and 300 K irradiations. The conservation of the η_{12} value between 77 K and 300 K is consistent with the stability of the arsenic vacancies, which has been previously suggested [1]. A previous study [27] indicates that after electron irradiation, the E_1 and E_2 defects may recover between 77 K and 300 K, probably as a result of the internal recombination of plural defects: in the simulation uncertainty limit, such recovering is not observed after swift ion irradiation. For the other acceptor defects, the conservation of the η_{AI} value between 77 K and 300 K does not necessarily mean the conservation of each defect: it is possible that the nature of some defects has changed, but with an identical charge state. Besides, we point out that, between 77 K and 300 K, defect conservation is not proved for neutral defects because they are ignored in our simulations.

Different ions with various incident energies were used for the irradiations of epitaxial GaAs. For the investigated ions, the experimental variations of n_H and μ_H as a function of fluence can be scaled between them by constant factors. So the results obtained during irradiation with oxygen and xenon at 77 K can be simulated with the same calculation models as for krypton. Adopting donor-acceptor $(-/0/+)$ charge states of the arsenic vacancy, the obtained defect creation rate values are reported in Table I for all experiments. All the simulations give constant values for the introduction rate ratios η_{12}/η_{AI}, which means that the investigated ions, with different energies, produce the same qualitative damage in the material and differ only by their defect production efficiency.

5. Discussion of Electronic Stopping Power Effect

Irradiation induced electronic excitation, which is due to the incident ion energy deposition, may have two contradictory consequences in defect production: either creation of defects, or annealing of defects To estimate the incidence of electronic excitation, it is useful to compare the sum of the creation rates appearing in our simulation, $\Sigma\eta_i = \eta_{12} + \eta_{AI}$, with the atomic displacement rate due only to nuclear collisions, without taking electronic excitation into account. The atomic displacement rate is the number of matrix atoms displaced by each incident ion, per unit length of its course. When it is due to nuclear collisions, this rate is labelled $Ndpa/e$ and can be estimated theoretically with Monte-Carlo type computation such as TRIM (Transport of Ions in Matter [28]) With TRIM, we have calculated $Ndpa/e$ and the electronic stopping power S_e for all experiments, the obtained values are listed in Table I. It can be seen that the experimental $\Sigma\eta_i$ value is approximately 50% of the theoretical $Ndpa/e$ value Thus, it seems that nuclear collisions are sufficient to interpret the quantity of produced defects· the 50% of undetected displacements may correspond to recombined primary defects (gallium vacancy-interstitial pairs for example) or to defects created in neutral charge states (deep donors). In all cases, the very large energy which is deposited in electronic excitation seems to be inefficient in defect creation, even for S_e values as large as 11.6 MeV/μm.

Depending on the irradiated material, the electronic stopping power may have various consequences [9]. For low S_e values, electronic excitation results simply in heat production without any consequence for defect creation. In some materials, specific effect may appear above a S_e threshold value of some MeV/μm. Spectacular electronic excitation induced damage production was observed in some metals [7]: such effect may be explained by several mechanisms, due either to thermal spike [29] or to electrostatic repulsion explosion [30] in the ion wake. However, when no spectacular effect can be detected, it is difficult to make electronic excitation influence evident, because the S_e variation scales approximately with the S_n variation. S_e influence on defect production may be concluded if large difference between experimental creation rates and S_n induced creation rates is observed: it is shown in the present study that this is not the case for GaAs. Electronic excitation effect generally appears over a certain S_e threshold: then S_e influence may be concluded if experimental creation rate *versus* $Ndpa/e$ variation is not linear. Previous studies realized on Ge and GaAs thinned samples have suggested that, for highest S_e values (20–35 MeV/μm), electronic excitation produces a partial annealing of defects created by nuclear collisions· this small effect could be seen in the bending of curves representing experimental damage production *versus* $Ndpa/e$ [15,16]. To study this possibility in the case of our epitaxial samples, we plot $\Sigma\eta_i$ *versus* $Ndpa/e$ (Fig. 9). The observed variation is practically linear, which means that no annealing effect can be evidenced here for $S_e \leq 11.6$ MeV/μm.

A final comment comes from the comparison of 77 K and 300 K irradiation results. Several papers indicate that, after electron irradiation, metastable defects may be annealed or

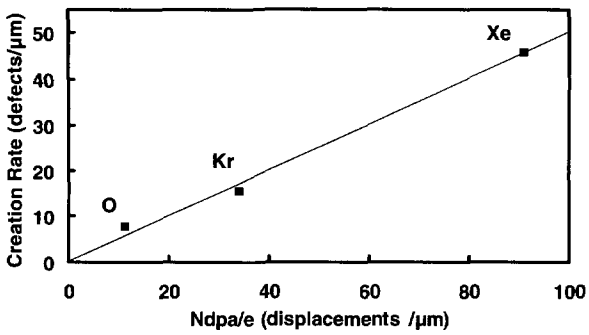

Fig. 9. — Sum of defect creation rates ($\eta_{12} + \eta_{A1}$), obtained from experimental result simulations, *versus* theoretical atomic displacement rate ($Ndpa/e$) calculated by TRIM computation. The three dots correspond respectively to oxygen, krypton and xenon irradiations.

regenerated between 77 K and 300 K, then inducing stable defect recovering [27, 31]. In our swift ion irradiation study, we observe the conservation of the defect creation rates. In this case, a possible explanation is that the electronic excitation could be effective in annealing the metastable defects already at 77 K· only the stable defects would then mainly control the compensation at both temperatures, 77 K and 300 K. The straight line observed in Figure 9 would then mean that the stable defect creation rate is proportional to $Ndpa/e$.

6. Conclusion

With a simple model, assuming that band tailing for large doping is represented by discrete impurity band conduction, it is possible to simulate the electronic characteristics of n- type epitaxial GaAs samples, particularly during swift ion irradiation. In that way, for 77 K irradiations, we could simulate the variations of both Hall concentration and Hall mobility *versus* fluence. However, for 300 K irradiations, the model, which uses the Matthiessen rule, only allows the variation of n_H to be simulated. Despite its simplicity, this model allows the differentiation of the various hypothesis concerning arsenic vacancy charge states: the observed results corroborate the most recently affirmed assumption of two levels E_1 and E_2 corresponding, respectively, to the single acceptor and to the single donor transitions of V_{As}.

The simulations of n_H variations, for 77 K and 300 K irradiations, indicate that the magnitudes of generated charged defects are similar at these two temperatures: this is particularly consistent with the fact that the arsenic vacancy, the main point defect created by swift ion irradiation, is stable at these temperatures.

Furthermore, the total experimental charged defect production rate represents approximately 50% of the theoretical atomic displacement rate due only to nuclear collisions. It appears that the large electronic excitation, which is induced in the material by swift ion irradiation, does not produce any effect in damaging, neither stable defect creation, nor annealing. This result, which is obtained here for the irradiation of epitaxial GaAs by various ions with $S_e \leq 11\ 6$ MeV/μm, seems to be different from previously reported results obtained for thinned GaAs samples [13, 16], where a weak annealing effect was concluded, particularly with ions presenting higher values of S_e. To state whether this discrepancy is apparent or due to the difference between the two materials, an additional experiment would be needed: epitaxial GaAs should be irradiated by ions with very high S_e values (20 – 30 MeV/μm)

References

[1] Pons D. and Bourgoin J.C., Irradiation-induced defects in GaAs, *J. Phys. C: Solid State Phys.* **18** (1985) 3839-3871.

[2] Loualiche S., Nouailhat A., Guillot G. and Lannoo M., Interpretation of deep-level optical spectroscopy and deep-level transient spectroscopy data: Application to irradiation defects in GaAs, *Phys. Rev. B* **30** (1984) 5822-5834.

[3] Look D.C., The donor nature of the main electron traps in electron-irradiated n-type GaAs, *Solid State Commun.* **64** (1987) 805-807.

[4] Corbel C., Positron annihilation and charge state of the vacancies in as-grown and electron irradiated GaAs, *Nucl. Instrum. and Methods B* **63** (1992) 166-172.

[5] Ziebro B., Hemsky J W. and Look D.C., Defect models in electron-irradiated n-type GaAs, *J. Appl. Phys.* **72** (1992) 78-81.

[6] Auret F.D , Goodman S.A., Myburg G., Barnard W.O. and Jones D.T.L , Electrical characterization of neutron irradiation induced defects in undoped epitaxially grown n-GaAs. *J. Appl. Phys.* **74** (1993) 4339-4342.

[7] Dunlop A and Lesueur D., Damage creation via electronic excitations in metallic targets, part I: experimental results, *Rad. Effects and Defects in Solids.* **126** (1993) 123-128.

[8] Dunlop A., Lesueur D., Legrand P., Dammak H and Dural J., Effects induced by high electronic excitations in pure metals: a detailed study in iron, *Nucl. Instrum and Methods B* **90** (1994) 330-338

[9] Balanzat E., Heavy ion induced effects in materials, *Rad. Effects and Defects in Solids.* **126** (1993) 97-104.

[10] Mary P., Bogdanski P., Nouet G and Toulemonde M., Defects created by 3.5 GeV xenon ions in silicon, *Appl. Surf. Sci.* **43** (1989)102-105.

[11] Marie P , Levalois M. and Bogdanski P., Deep level transient spectroscopy of high-energy heavy ion irradiation-induced defects in n-type germanium, *J. Appl. Phys.* **74** (1993) 868-871

[12] Marie P. and Levalois M., Hole traps produced by swift heavy ion irradiation in p-type germanium, *J. Appl. Phys.* **75** (1994) 1852-1854.

[13] Mikou M., Carin R., Bogdanski P. and Madelon R , Experimental study by *in situ* resistivity measurements of swift heavy ion induced defects in GaAs crystals, *Nucl. Instrum and Methods B* **107** (1996) 246-249.

[14] Levalois M., Bogdanski P. and Toulemonde M., Induced damage by high energy heavy ion irradiation at the GANIL accelerator in semiconductor materials, *Nucl. Instrum and Methods B* **63** (1992) 14-20.

[15] Levalois M., Girard J.P., Allais G., Hairie A., Metzner M.N. and Paumier E., High energy ion irradiation of germanium, *Nucl. Instrum and Methods B* **63** (1992) 25-29.

[16] Carin R., Madelon R., Julienne D., Cruege F. and Hairie A., An investigation by resistance and photoluminescence measurements of high-energy heavy-ion irradiated GaAs, *Nucl. Instrum and Methods B* **63** (1992) 21-24.

[17] Marie P., Levalois M. and Paumier E., Swift-heavy-ion induced damage in germanium: An evaluation of defect introduction rates, *J. Appl. Phys.* **79** (1996) 7555-7562.

[18] Look D.C., Electrical Characterization of GaAs Materials and Devices (Wiley, 1989) pp. 1-131.

[19] Stillman G.E and Wolfe C.M., Electrical characterization of epitaxial layers, *Thin Sol. Films* **31** (1976) 69-88.

[20] Lowney J R., Impurity bands and band tailing in n-type GaAs, *J. Appl. Phys.* **60** (1986) 2854-2859.

[21] Benzaquen M . Mazuruk K., Walsh D., Blaauw C. and Puetz N., Electrical characteristics of III-V compounds grown by MOVPE, *J. Cryst. Growth* **77** (1986) 430-436.

[22] van der Pauw L.J , A method of measuring specific resistivity and Hall effect of discs of arbitrary shape, *Philips Res. Rep.* **13** (1958) 1-9

[23] Benzaquen M., Walsh D. and Mazuruk K., Hall factor of doped n-type GaAs and n-type InP, *Phys. Rev. B* **34** (1986) 8947-8949.

[24] Walukiewicz W., Lagowski L., Jastrzebski L., Lichtensteiger M. and Gatos H.C., Electron mobility and free-carrier absorption in GaAs: Determination of the compensation ratio, *J. Appl. Phys.* **50** (1979) 899-908.

[25] Erginsoy C., Neutral impurity scattering in semiconductors, *Phys. Rev.* **79** (1950) 1013-1014.

[26] Rode D.L. and Knight S , Electron transport in GaAs, *Phys Rev. B* **3** (1971) 2534-2541.

[27] Rezazadeh A A. and Palmer D.W., An electron-trapping defect level associated with the 235 K annealing stage in electron-irradiated n-GaAs, *J. Phys. C: Solid State Phys.* **18** (1985) 43-54.

[28] Biersack J.P. and Haggmark L.G , A Monte Carlo computer program for the transport of energetic ions in amorphous targets, *Nucl. Instrum and Methods* **174** (1980) 257-269.

[29] Toulemonde M., Paumier E and Dufour C., Thermal spike model in the electronic stopping power regime, *Rad. Effects and Defects in Solids* **126** (1993) 201-206.

[30] Lesueur D. and Dunlop A., Damage creation via electronic excitations in metallic targets, part II: a theoretical model, *Rad. Effects and Defects in Solids* **126** (1993) 163-172.

[31] Hesse M., Koschnick F.K., Krambrock K. and Spaeth J.-M., Metastability of arsenic antisite-related defects created by electron irradiation in gallium arsenide, *Solid State Commun.* **92** (1994) 207-211.